2950 *Chem. Mater.* **2009,** *21,* 2950–2956
DOI:10.1021/cm9006603

CHEMISTRY OF MATERIALS
Article

Hydrothermal Dehydration for the "Green" Reduction of Exfoliated Graphene Oxide to Graphene and Demonstration of Tunable Optical Limiting Properties

Yong Zhou, Qiaoliang Bao, Lena Ai Ling Tang, Yulin Zhong, and Kian Ping Loh*

Department of Chemistry, National University of Singapore (NUS), 3 Science Drive 3, 117543, Singapore

Received March 7, 2009. Revised Manuscript Received April 19, 2009

This work reports a simple, clean, and controlled hydrothermal dehydration route to convert graphene oxide (GO) to stable graphene solution. The hydrothermally treated GO was characterized using UV−visible absorption spectroscopy, atomic force microscopy, Raman spectroscopy, X-ray photoemission spectroscopy, and solid state ^{13}C NMR spectra. Compared to chemical reduction processes using hydrazine, the present "water-only" route has the combined advantages of removing oxygen functional groups from GO and repairing the aromatic structures. By controlling the hydrothermal temperatures, we can modify the physical properties of GO and obtain tunable optical limiting performance.

Introduction

Graphene (G), a single aromatic sheet of sp^2 bonded carbon, exhibits novel electronic properties such as ballistic transport, massless Dirac fermions,[1] Berry's phase,[2] high conductivity,[3] and localization suppression.[4] Recently, there have been intense efforts to apply graphene materials in electronic, optoelectronic, capacitor, and sensing applications. This is driven by the desire to discover a new performance threshold in this novel material.[5−14] Among the current methods of generating graphene, solution-processed routes offer the greatest ease for functionalization and bulk-scale processing. Solution-processed graphene can be conveniently applied for spin-coating or inkjet-printing on plastic substrates; therefore, it has the potential to realize large scale organic devices or photovoltaic cells. One problem is that the carrier mobility in solution-processed graphene is orders of magnitude poorer than the mechanically cleaved graphene due to the presence of a large amount of defects.[15] It is also nontrivial to produce graphene films of uniform thickness (e.g., monolayer) over a large area because the hydrophobic graphene has a strong tendency to agglomerate in aqueous solvents. Exfoliation of graphite via oxidation with strong acids is one way to generate bulk quantities of graphene oxide (GO) which can form stable suspension in water.[16] However, the reduction of GO to graphene is necessary to recover the conjugated network and electrical conductivity.[17] The carboxyl, hydroxyl, or epoxy groups bonded on graphene and other atomic-scale lattice defects modify the electronic structure of G and serve as strong scattering centers that can affect the electrical transport and light transmission.[18] Currently,

*Corresponding author. Tel: (65) 6516 4402. Fax (65) 6779 1691. E-mail: chmlohkp@nus.edu.sg.

(1) Novoselov, K. S.; Geim, A. K.; Morozov, S. V.; Jiang, D.; Katsnelson, M. I.; Grigorieva, I. V.; Dubonos, S. V.; Firsov, A. A. *Nature* **2005**, *438*, 197.
(2) Zhang, Y.; Tan, Y. W.; Stormer, H. L.; Kim, P. *Nature* **2005**, *438*, 201.
(3) Geim, A. K.; Novoselov, K. S. *Nat. Mater.* **2007**, *6*, 183.
(4) Morozov, S. V.; Novoselov, K. S.; Katsnelson, M. I.; Schedin, F.; Ponomarenko, L. A.; Jiang, D.; Geim, A. K. *Phys. Rev. Lett.* **2006**, *97*, 016801/1.
(5) (a) Standley, B.; Bao, W.; Zhang, H.; Bruck, J.; Lau, C. N.; Bockrath, M. *Nano Lett.* **2008**, *8*, 3345. (b) Gilje, S.; Han, S.; Wang, M.; Wang, K. L.; Kaner, R. B. *Nano Lett.* **2007**, *7*, 3394. (c) Gomez-Navarro, C.; Weitz, R. T.; Bittner, A. M.; Scolari, M.; Mews, A.; Burghard, M.; Kern, K. *Nano Lett.* **2007**, *7*, 3499.
(6) Robinson, J. T.; Perkins, F. K.; Snow, E. S.; Wei, Z.; Sheehan, P. E. *Nano Lett.* **2008**, *8*, 3137.
(7) (a) Chen, J. H.; Ishigami, M.; Jang, C.; Hines, D. R.; Fuhrer, M. S.; Williams, E. D. *Adv. Mater.* **2007**, *19*, 3623. (b) Wu, Y. Q. *Appl. Phys. Lett.* **2008**, *92*, 092102.
(8) (a) Liu, Q.; Liu, Z.; Zhang, X.; Zhang, N.; Yang, L.; Yin, S.; Chen, Y. *Appl. Phys. Lett.* **2008**, *92*, 223303. (b) Wang, X.; Zhi, L. J.; Tsao, N.; Tomovic, Z.; Li, J. L.; Mullen, K. *Angew. Chem., Int. Ed.* **2008**, *47*, 2990. (c) Becerril, H. A.; Mao, J.; Liu, Z. *ACS Nano* **2008**, *2*, 463. (d) Wang, X.; Zhi, L. J.; Mullen, K. *Nano Lett.* **2008**, *8*, 323.
(9) (a) Mohanty, N.; Berry, V. *Nano lett.* **2008**, *8*, 4469. (b) Lu, J.; Do, I.; Drzal, L. T.; Worden, R. M.; Lee, I. *ACS Nano* **2008**, *2*, 1825.
(10) Stoller, M. D.; Park, S.; Zhu, Y.; An, J.; Ruoff, R. S. *Nano Lett.* **2008**, *8*, 3498.
(11) Yoo, E.; Kim, J.; Hosono, E.; Zhou, H.; Kudo, T.; Honma, I. *Nano Lett.* **2008**, *8*, 2277.
(12) Liu, Z.; Robinson, J. T.; Sun, X.; Dai, H. *J. Am. Chem. Soc.* **2008**, *130*, 10876.
(13) (a) Stankovich, S.; Dikin, D. A.; Dommett, G. H. B.; Kohlhaas, K. M.; Zimney, E. J.; Stach, E. A.; Piner, R. D.; Nguyen, S. T.; Ruoff, R. S. *Nature* **2006**, *442*, 282. (b) Watcharotone, S.; Dikin, D. A.; Stankovich, S.; Piner, R.; Jung, I.; Dommett, G. H. B.; Evmenenko, G.; Wu, S. E.; Chen, S. F.; Liu, C. P.; Nguyen, S. T.; Ruoff, R. S. *Nano Lett.* **2007**, *7*, 1888. (c) Yu, A. P.; Ramesh, P.; Itkis, M. E.; Bekyarova, E.; Haddon, R. C. *J. Phys. Chem. C* **2007**, *111*, 7565. (d) Becerril, H. A.; Mao, J.; Liu, Z.; Stoltenberg, R. M.; Bao, Z.; Chen, Y. *ACS Nano* **2008**, *2*, 463.
(14) Ang, P. K.; Chen, W.; Wee, A. T. S.; Loh, K. P. *J. Am. Chem. Soc.* **2008**, *130*, 14392.
(15) Palacios, J. J.; Fernández-Rossier, J. *Phys. Rev. B* **2008**, *77*, 195428.
(16) Laura, J. C.; Franklin, K.; Huang, J. *J. Am. Chem. Soc.* **2009**, *131*, 1043.
(17) Li, D.; Muller, M. B.; Gilje, S.; Kaner, R. B.; Wallace, G. G. *Nat. Nanotechnol.* **2007**, *3*, 101.
(18) Rutter, G. M.; Crain, J. N.; Guisinger, N. P.; Li, T.; First, P. N.; Stroscio, J. A. *Science* **2007**, *317*, 219.

Published on Web 05/26/2009

reducing agents such as hydrazine and dimethylhydrazine are widely used for the chemical reduction of GO to graphene.[17,19−25] In view of the fact that hydrazine is toxic and dangerously unstable, it is desirable to explore a green chemistry route for the reduction of graphene.

Supercritical water (SC) can play the role of reducing agent in hydrothermal conditions and offers a green chemistry alternative to organic solvents. In addition, its physiochemical properties can be changed widely with pressure and temperature. SC water behaves like a water-like fluid with strong electrolytic solvent power, high diffusion coefficient, high ion molecules, and a dielectric constant that can be comparable with that of polar organic molecules. These properties allow the catalysis of a variety of heterolytic (ionic) bond cleavage reactions in water. Hydrothermal routes have been employed for remarkable transformation of carbohydrate molecules to form homogeneous carbon nanospheres[26−28] and nanotubes.[29]

In this paper, we explore a simple hydrothermal route to convert GO to stable graphene suspension in water. The hydrothermal conversion method has several advantages over the common chemical reduction processes: (1) the process requires very simple setup, that is, basically an autoclave; (2) it has good upward scalability and is industrially compatible with batch processing; (3) it is intrinsically pure because it utilizes only water, as opposed to the hydrazine or sulfonate chemical reduction method which inevitably introduces noncarbon impurities into the treated GO;[30] (4) the closed system of relative high temperature and internal pressure promotes the recovery of π-conjugation after dehydration, which is favorable for minimizing defects;[25] and (5) engineering the parameters of temperature and pressure affords a facile method to control the degree of reduction of the GO. As a proof of principle for point (4), we demonstrate that GO with different degrees of hydrothermal reduction has its electronic and optical properties modified sufficiently to display distinct optical transmittance and limiting properties.

Experimental Section

GO was prepared using a modified Hummers method from graphite powders (Grade 230 U kindly presented by Asbury Graphite Mills Inc., Kittunning, Pa).[16] A total of 25 mL of 0.5 mg/mL GO aqueous solution was transferred to a Teflon-lined autoclave and heated at 180 °C for 6 h. The autoclave was then cooled to room temperature. The hydrothermally treated graphene was found to precipitate at the bottom of the autoclave as a black powder, possibly due to the low solubility in superfluidic water under hydrothermal conditions. The graphene could be readily dispersed by ultrasonification in water. The pH of the solution was adjusted with hydrochloric acid and ammonia solution.

Hydrazine-reduced GO was obtained by adding 10 mL of 98% hydrazine solution into 10 mL of 0.5 mg/mL GO solution. The reduction proccess was carried out at 50 °C for 12 h. The graphene flakes were collected with filtration, washed with pure water several times, and dried at 90 °C.

Characterization. Field emission-secondary electron microscope (FE-SEM) images were carried out with a FE scanning electron microanalyzer (JEOL-6300F, 5 kV). The UV−vis absorption spectra were recorded on a Shimadzu UV 2450PC spectrophotometer. AFM images were taken with Dimension 3100, Digital Instruments, Veeco Metrology Group. The $I-V$ curve was obtained by two-point measurement using a Keithley 6430 Subfemtoamp remote sourcemeter on a REL-3200 probe station. Raman spectroscopy was carried out using a WITEC CRM200 Raman system.[31] The excitation source is a 532 nm laser (2.33 eV) with a laser power below 0.1 mW on the sample to avoid laser-induced local heating. A 100 objective lens with a numerical aperture (NA) of 0.95 was used in the Raman experiments, and the spot size of a 532 nm laser was estimated to be 500 nm. The spectra resolution of our Raman system is 1 cm^{-1}. XPS was performed with a Phobios 100 electron analyzer (SPECS GmbH) equipped with 5 channeltrons, using an unmonochromated Al Kα Xray source (1486.6 eV). The pass energy of the hemisphere analyzer was set at 50 eV for wide scan and 20 eV for narrow scan, while the takeoff angle was fixed at normal to the sample. High-resolution solid-state ^{13}C NMR experiments were carried out on a Bruker DRX-400 MHz NMR spectrometer.

Optical Measurements. Monolayer GO and graphene (G) nanosheets were electrostatically assembled on the optical fiber using a layer-by-layer technique for optical studies;[17] that is, a self-assembled polyethyleneimine (PEI) monolayer was first formed on SiO_2 followed by immersing the substrate into dilute GO or G aqueous solutions to obtain monolayer GO or G thin films. Two layers of GO or G films were typically assembled, with thickness in the range of 2−3 nm. The nonlinear optical properties including optical limiting, nonlinear transmission, and absorbance measurements were performed using 1560 nm infrared fiber laser irradiation (spot size: 5 μm) with either continuous wave or 5 ns pulses (100 MHz repetition rate).

(19) Stankovich, S.; Piner, R. D.; Chen, X.; Wu, N.; Nguyen, S. T.; Ruoff, R. S. *J. Mater. Chem.* **2006**, *16*, 155.
(20) Si, Y.; Samulski, E. T. *Nano Lett.* **2008**, *8*, 1679.
(21) (a) Niyogi, S.; Bekyarova, E.; Itkis, M. E.; McWilliams, J. L.; Hamon, M. A.; Haddon, R. C. *J. Am. Chem. Soc.* **2006**, *128*, 7720. (b) Wang, S.; Chia, P.; Chua, L.; Zhao, L.; Png, R.; Sivaramakrishnan, S.; Zhou, M.; Goh, R. G. S.; Friend, R. H.; Wee, A. T. S.; Ho, P. K. H. *Adv. Mater.* **2008**, *20*, 3440.
(22) Tung, V. C.; Allen, M. J.; Yang, Y.; Kaner, R. B. *Nat. Nanotechnol.* **2009**, *4*, 25.
(23) Fan, X.; Peng, W.; Li, Y.; Li, X.; Wang, S.; Zhang, G.; Zhang, F. *Adv. Mater.* **2008**, *20*, 4490.
(24) Xu, Y.; Bai, H.; Lu, G.; Li, C.; Shi, G. *J. Am. Chem. Soc.* **2008**, *130*, 5856.
(25) Li, X.; Zhang, G.; Bai, X.; Sun, X.; Wang, X.; Wang, E.; Dai, H. *Nat. Nanotechnol.* **2008**, *3*, 538.
(26) Sun, X.; Li, Y. *Angew. Chem., Int. Ed.* **2004**, *43*, 597.
(27) (a) Shin, Y.; Wang, L. Q.; Bae, I. T.; Arey, B. W.; Exarhos, G. J. *J. Phys. Chem. C* **2008**, *112*, 14236. (b) Yao, C.; Shin, Y.; Wang, L.; Windisch, C. F.; Samuels, W. D. Jr.; Arey, B. W.; Wang, C.; Risen, W. M.; Exarhos, G. J. Jr. *J. Phys. Chem. C* **2007**, *111*, 15141.
(28) Zhang, L.; Fu, H.; Zhu, Y. *Adv. Funct. Mater.* **2008**, *18*, 2180.
(29) (a) Gong, J.; Luo, L.; Yu, S.; Qian, H.; Fei, L. *J. Mater. Chem.* **2006**, *16*, 101. (b) Qian, H.; Luo, L.; Gong, J.; Yu, S.; Li, T.; Fei, L. *Cryst. Growth Des.* **2006**, *6*, 607. (c) Luo, L.; Yu, S.; Qian, H.; Zhou, T. *J. Am. Chem. Soc.* **2005**, *127*, 2822.
(30) Stankovich, S.; Dikin, D. A.; Piner, R. D.; Kohlhaas, K. A.; Kleinhammes, A.; Jia, Y.; Wu, Y.; Nguyen, S. T.; Ruoff, R. S. *Carbon* **2007**, *45*, 1558.
(31) (a) Ni, Z.; Wang, Y.; Yu, T.; You, Y.; Shen, Z. *Phys. Rev. B* **2008**, *77*, 235403. (b) Ni, Z.; Wang, H. Z.; Kasim, J.; Fan, H. M.; Yu, T.; Wu, Y. H.; Feng, Y. P.; Shen, Z. X. *Nano Lett.* **2007**, 2758.

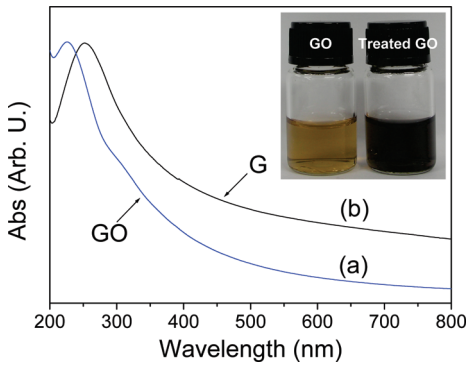

Figure 1. UV−vis absorption spectra of the GO (a) before and (b) after hydrothermal treatment at 180 °C for 6 h. Inset shows the color change of 0.5 mg/mL GO solution before and after hydrothermal treatment.

Results and Discussion

Superheated H_2O promotes acid-catalyzed reaction of organic compounds because of a sufficiently high H^+ concentration compared to normal liquid phase. Therefore, the hydrothermal reduction was first carried out using neutral water. The UV−vis absorption spectra show that the absorption peak (227 nm) of GO corresponding to $\pi \rightarrow \pi^*$ transitions of aromatic C=C bonds red-shifts to 254 nm after hydrothermal reduction treatment at 180 °C for 6 h (Figure 1). The absorption in the whole spectral region (> 238 nm) increases, which is indicative of the restoration of the π-conjugation network within the G nanosheets. The inset shows the color change of 0.5 mg/mL GO solution from yellow brown to black after hydrothermal treatment. The black color is evident of the partial restoration of the conjugation network within the carbon structure.

The pH dependence of the hydrothermal reaction was investigated next. We found that hydrothermal dehydration of the GO solution at pH = 11 yielded a stable G solution which can be subsequently spin-coated as single layer G film (Figure 2a). However, treatment of GO solution at pH = 3 resulted in intense aggregation of G, which cannot be dispersed well even in concentrated ammonia solution. The reduction process is believed to be analogous to the H^+-catalyzed dehydration of alcohol, where water acts as a source of H^+ for the protonation of OH. As illustrated in Scheme 1, both intramolecular as well as intermolecular dehydration can occur on the edges or basal planes of G. The edges of the GO, as well as some parts of its basal plane, are terminated by hydrogen, hydroxyl, ether, and carboxylic groups. In the case of intramolecular dehydration, the elimination of OH and H can occur on the edge sites of G, followed by the recovery of π-bonding. As a result of the principle of microscopic reversibility, the acid-catalyzed dehydration has a reverse mechanism, that is, the acid-catalyzed hydration. This is a reversible reaction, and not all oxygen groups can be removed from the G at the end of the reaction. As a result, the residual negatively charged oxygen functional groups allow the G solution to be dispersed well in water. Using neutral water as the reacting solvent, the suspension remains stable for three days.[17,22,23]

Scheme 1. (a) Intramolecular Dehydration of G Catalyzed by H^+ [a] and (b) Intermolecular Dehydration of G Occuring at High pH, Giving Rise to Aggregated Products

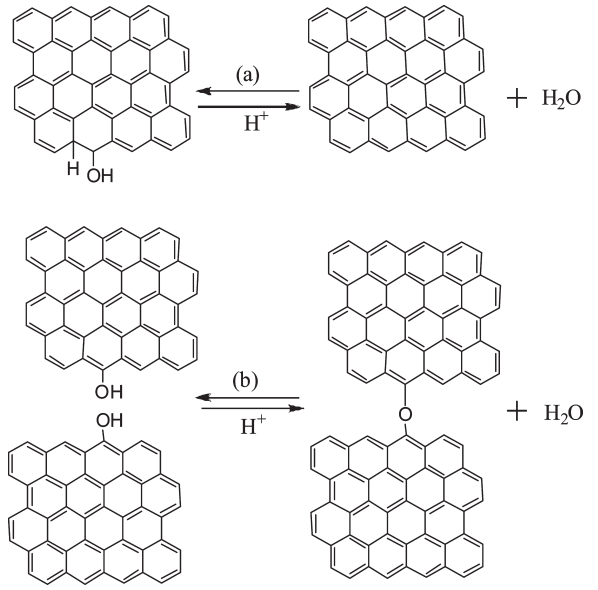

[a] Symbolic H and OH functional groups were drawn terminating the edges of G.

The role of pH is important in the dispersion of the reduced G. In highly acidic media, the zeta potential of GO is small[17,23] because of the protonation of the O^- and COO^- group on GO. In this case the electrostatic repulsion between the GO sheets is not strong enough to overcome the aggregation of the GO by noncovalent interactions, that is, $\pi-\pi$ interactions or H-bonding. In the aggregated state, the material has a tendency to undergo intermolecular dehydration catalyzed by H^+, leading to the coupling of G via ether linkages. These are covalently coupled G because subsequent ultrasonication in concentrated alkali cannot disperse these strongly bound covalently bound agglomerates. In contrast, in alkali media, the zeta potential of the GO (> −43 mV) is high due to the presence of negatively charged O^- and COO^- groups. In such a case, the GO is well dispersed as a result of electrostatic repulsion and intramolecular dehydration occuring on the edges of the GO instead.

The AFM image reveals that the thickness of the G sheet obtained is about 0.8 nm (Figure 2a). This value is smaller than that of as-used GO of about 1.5 nm (Figure 2b), which could be explained by the removal of the surface oxide groups. The thickness is also thinner than those of chemically converted G, which is generally larger than 1.0 nm. Field-emission scanning electron microscopic (FE-SEM) images of the hydrothermally treated GO demonstrate that the 2-D molecular sheet was well preserved for hydrothermal reactions carried out at neutral or alkaline pH (Figure 2c). The G was thin enough to be flexible and restack to some degree upon freeze-drying (Figure 2d). The absence of charging during

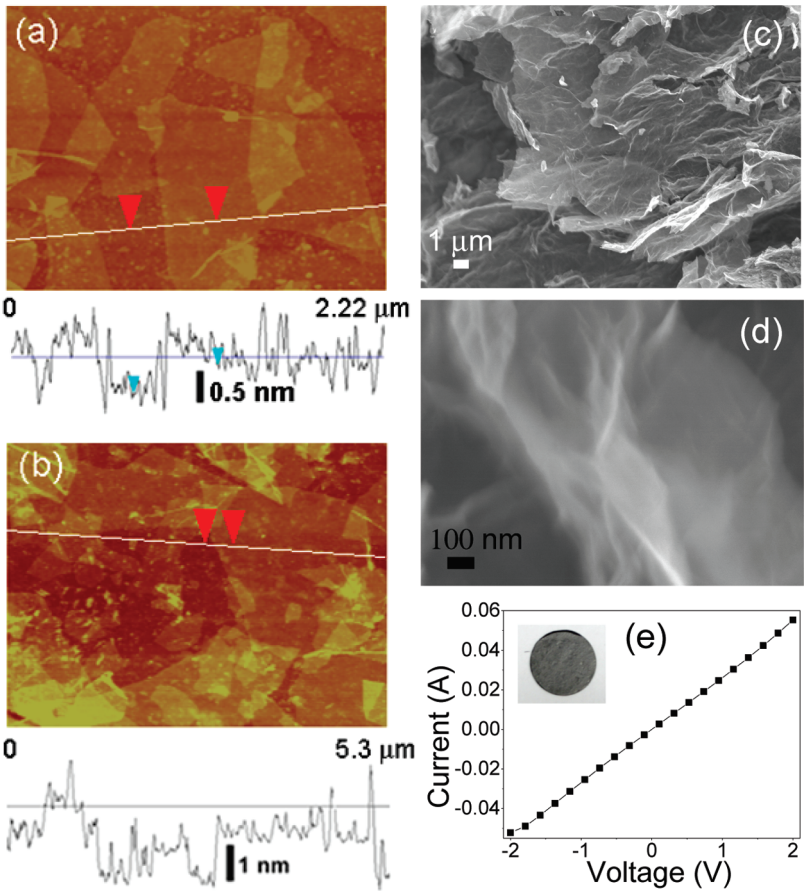

Figure 2. (a and b) AFM images of G and GO after and before hydrothermal treatment at 180 °C for 6 h, respectively, and the corresponding section analyses; (c and d) FE-SEM images at different magnification of the G; and (e) the room-temperature $I-V$ curve of the G disk, exhibiting ohmic characteristics. The G disk was prepared by pressing the powder into the pellet with a hydraulic press.

the SEM imaging indicates that the network of G-based sheets and the individual sheets are electrically conductive. Current−voltage measurement also confirms that the hydrothermally reduced G is conductive, compared to the insulating GO before treatment (Figure 2e).

High-resolution X-ray photoemission C 1s spectra (XPS) of the GO show a significant decrease of oxygenated carbon related signals at 286−289 eV after dehydration (Figure 3a), confirming that most of the epoxide, hydroxyl, and carboxyl functional groups were successfully removed. The molar ratio of sp^2 carbon to oxidized sp^3 carbon increases from 1.8 for GO to 5.6 for G. XPS wide scan of the surface of the hydrothermally treated sample showed that it was very pure and had no impurities, and the only elements present were oxygen and carbon. The solid state ^{13}C nuclear magnetic resonance (NMR) spectrum of the GO confirms the presence of abundant epoxide and hydroxyl groups (Figure 3b). The peaks at 59 and 69 ppm represent the ^{13}C nuclei in the epoxide and hydroxyl groups, respectively. The resonance at 126 ppm belongs to the unoxidized sp^2 carbons of the graphene network, and that at 183 ppm arises from the carbonyl groups. After the hydrothermal reaction, the amount of oxygen-containing functional groups of the treated GO was significantly reduced. In addition, the population of sp^2 carbon atoms increased, as indicated by the increase in the peak at 94−160 ppm, which is reflective of the dehydration/reduction reactions and recovery of π-conjugation.

Micro-Raman spectroscopy was used to characterize the GO before and after hydrothermal dehydration (Figure 4). For comparison, the Raman spectrum of hydrazine-reduced GO is also shown. The typical features in the Raman spectra are the G band at 1593 cm^{-1} and the D band at 1352 cm^{-1} (Figure 4a). The G band is usually assigned to the E_{2g} phonon of C sp^2 atoms, while the D band is a breathing mode of κ-point phonons of A_{1g} symmetry. A prominent D band is an indication of disorder in the Raman of the GO, originating from defects associated with vacancies, grain boundaries,[32,33] and amorphous carbon species.[34] The intensity ratio (I_D/I_G) of D band to G band of the GO is about 0.96. Hydrothermal treatment at 180 °C for 6 h decreased the I_D/I_G to 0.90 (Figure 4b). This suggests that the hydrothermal reaction, besides dehydrating/reducing the GO, is also able to recover the aromatic structures by repairing defects. It is instructive to note that for hydrazine-reduced

(32) Tuinstra, F.; Koenig, J. L. *J. Chem. Phys.* **1970**, *53*, 1126.
(33) (a) Ferrari, A. C.; Meyer, J. C.; Scardaci, V.; Casiraghi, C.; Lazzeri, M.; Mauri, F.; Piscanec, S.; Jiang, D.; Novoselov, K. S.; Roth, S.; Geim, A. K. *Phys. Rev. Lett.* **2006**, *97*, 187401. (b) Ferrari, A. C.; Robertson, J. *Phys. Rev. B* **2000**, *61*, 14095.
(34) Schönfelder, R.; Rümmeli, M. H.; Gruner, W.; Löffler, M.; Acker, J.; Hoffmann, V.; Gemming, T.; Büchner, B.; Pichler, T. *Nanotechnology* **2007**, *18*, 375601.

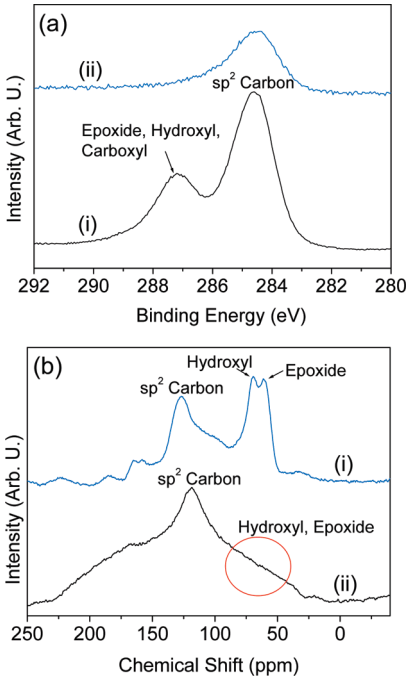

Figure 3. (a) XPS and (b) solid state ^{13}C NMR spectra of the GO, (i) before and (ii) after hydrothermal treatment at 180 °C for 6 h.

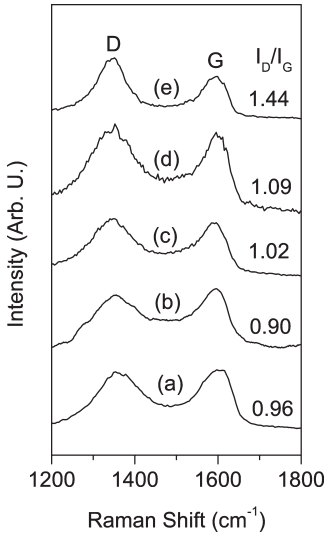

Figure 4. Raman spectra of (a) GO, G obtained with hydrothermal treatment of GO at (b) 180 °C, (c) 150 °C, and (d) 120 °C for 6 h, and (e) hydrazine-reduced GO.

G, the I_D/I_G ratio increased to 1.44 (Figure 4e) after treatment, and this is due to the presence of unrepaired defects that remained after the removal of oxygen moieties. This I_D/I_G ratio value is consistent with most chemical reduction reports. Therefore, we can conclude that the hydrothermal reduction route is more effective than the hydrazine reduction process in repairing the sp^2 network. Alteration of hydrothermal temperatures allows us to control the extent of conversion of GO to G. Specifically, treatment at 150 and 120 °C yielded G with I_D/I_G of 1.02 (Figure 4c) and 1.09 (Figure 4d), respectively. Considering the relationship of I_D/I_G with the extent of π-conjugation and concentration of defects on G, the present route allows the modification of the electronic or optical properties of G readily.

To test if the optical properties of G can be modified by the hydrothermal temperature, we explore the use of the hydrothermally reduced G as optical limiters when adsorbed on the end surface of an optical fiber. Optical limiters (OL) are devices designed to have high transmittance for low level inputs while blocking the transmittance for high intensity laser beams. Ideal OL should be effective for a broad range of laser exposure duration and repetitive rates, from subnanosecond pulse to continuous regime. We assembled the GO and G monolayers onto optical fibers using a layer-by-layer route[17] to explore their suitability as atomic layer OL. This approach, which directly tests the OL effects on atomic layers of G, is different from the conventional testing of OL effects which were usually carried out in solution. The advantage of this approach is that it allows the direct probing of the attenuation effects due to a well-defined thickness of GO or G, as opposed to solution testing where OL effects may arise from scattering effects by instantaneous bubbles created during the heating of the suspended material.[35] Figures 5a and 6a show the OL performance of the hydrothermally treated GO using 1560 nm continuous wave (CW) and nanosecond pulse laser irradiation, respectively. Figures 5b and 6b show the nonlinear absorbance versus laser intensity plot. For CW laser, the transmittance of 180 °C hydrothermally treated G is ~57%, and the output/input power ratio is 0.49. When the nanosecond pulsed laser was used, the transmittance decreased to ~12%, with an output/input power ratio of 0.11. The results indicate that the G derivative material here shows higher OL properties for nanosecond pulsed lasers compared to CW lasers.

Interestingly, the OL behavior of reduced GO differs depending on the hydrothermal treatment temperature as well as whether pulsed or continuous laser (CW) was used, attesting to the fact that the hydrothermal treatment can create significant variation in electronic and optical properties. As shown in Figure 5b, G produced by hydrothermal treatment at 150−180 °C exhibited better OL performance for CW laser compared to that treated at 120 °C and untreated GO. However, the OL performance was reversed in the case of nanosecond pulsed laser as shown in Figure 6b; that is, G treated at 120 °C as well as untreated GO exhibited better OL effects. The different OL mechanism arises from structures that have either the semiconductor (GO) or metallic (G) framework. At initial high CW laser intensity as shown in Figure 5b, the absorption actually decreases with laser intensity, and this is due to the occurrence of saturable absorption (SA). SA can arise when the first excited state has a lower absorption cross section compared to the ground state. For G generated by hydrothermal treatment at elevated temperatures, the repaired conjugated network affords a nearly zero-band gap condition which gives rise to a

(35) Riggs, J. E.; Walker, D. B.; Carroll, D. L.; Sun, Y. P. *J. Phys. Chem. B* **2000**, *104*, 7071.

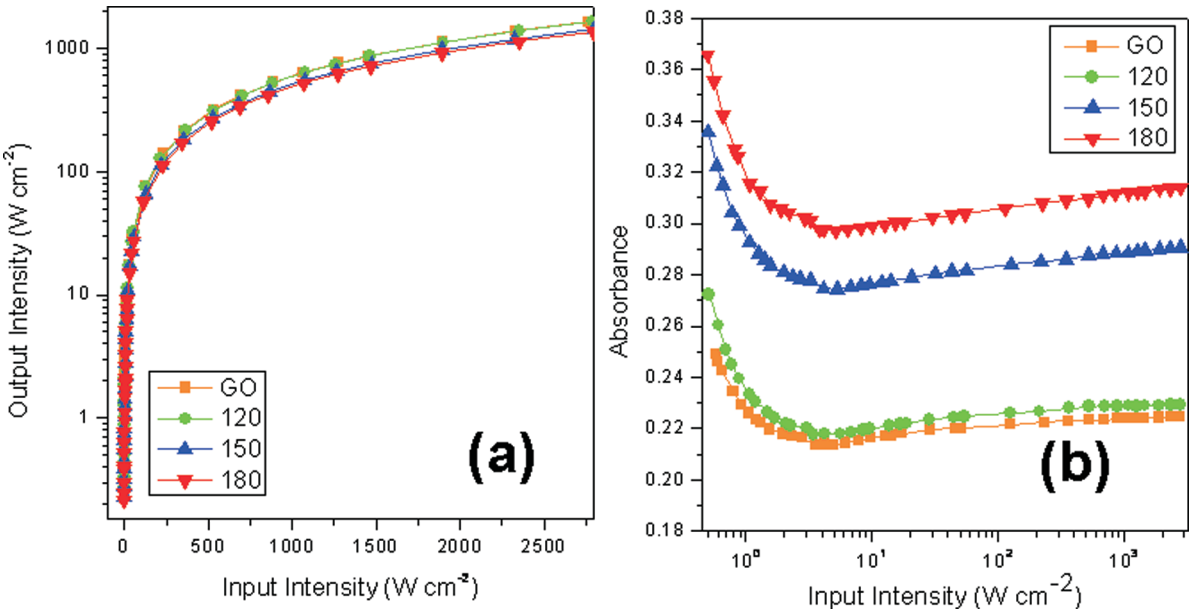

Figure 5. (a) Optical limiting (OL) performance of as-synthesized GO and GO after hydrothermal reduction, measured with continuous wave incident light (1560 nm); (b) nonlinear absorbance. Red line is due to pristine GO, and green, blue, and red lines are plots of GO hydrothermally treated at 120, 150, and 180 °C, respectively.

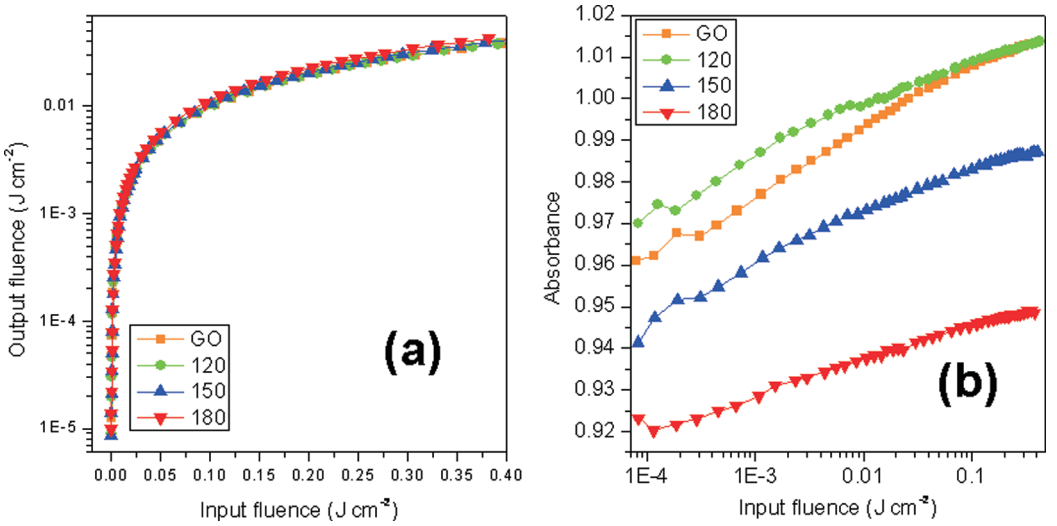

Figure 6. (a) Optical limiting (OL) performance of as-grown GO and GO after hydrothermal reduction, measured with 5 ns laser pulses (1560 nm). (b) Nonlinear absorbance. Red line is due to pristine GO, and green, blue, and red lines are plots of GO hydrothermally treated at 120, 150, and 180 °C, respectively.

higher initial adsorption as well as SA compared to partially reduced GO. At even higher laser intensity, reversed saturable absorption (RSA) occurs[36] and OL sets in. In the case of nanosecond pulsed laser as shown in Figure 6b, RSA dominates the entire range of laser fluence due to much stronger pulse energy. In this case, GO or partially reduced GO exhibits a greater OL effect than G, which may be associated with the presence of a finite band gap in these material which gives rise to greater proportions of excited state absorption.[35] The detailed mechanism needs further investigation, but the current work demonstrates that the optical transmittance and limiting properties are a sensitive function of the oxygen functional groups and structural defects in G.

Conclusion

A hydrothermal route toward clean and controlled reduction of GO to stable G solution was demonstrated. The present "water-based" route is advantageous compared to conventional chemical reduction processes using hydrazine because it is very convenient to use, environmentally friendly, and industrially scalable and shows the ability to recover aromatic structures via repairing the postreduction defects. We have also demonstrated that by controlling the hydrothermal treatment temperature, the optical properties of G can be modified. The hydrothermal route has unexplored potential because this work

(36) Liu, Z.; Wang, Y.; Zhang, X.; Xu, Y.; Chen, Y.; Tian, J. *Appl. Phys. Lett.* **2009**, *94*, 021902.

only utilized superheated water. By tuning the engineering parameters of temperature and pressure toward the supercritical point of water, the chemical properties of the water like dielectric constant and ion point will change, and the reduction chemistry may change in an interesting way. For future work, it is also possible to add haloacids like HBr or HCl so that conjugate base can undergo nucleophilic substitutions on G, thus affording a one-step hydrothermal reduction and functionalization.

Acknowledgment. The authors wish to acknowledge the NRF-CRP grant "Graphene Related Materials and Devices R-143-000-360-281" for the support of this project. Dr. Chen Xiaohong (NUS) is appreciated for the conductivity measurement, and Dr. Yang Jiaxiang (NUS) is also acknowledged for helpful discussion.